Biophysical Journal, Volume 99

Supporting Material

Neutron Reflectometry Study of the Conformation of HIV Nef Bound to Lipid Membranes

Michael Kent, Jaclyn Murton, Darryl Sasaki, Sushil Satija, Bulent, Akgun, Hirsh, Nanda, Joseph Curtis, Jaroslow Majewski, Christopher Morgan, and John Engen

Spectral data for d-DSIDA (d70)

[^{1}H NMR ($CDCl_3$) δ 3.69 (m, 4H, -NC*H*$_2$CO-), 3.64 – 3.41 (m, 21H, -C*H*$_2$O-), 3.05 (br s, 2H, -NC*H*$_2$-), 1.21 (m, 3H, -C*H*-). ^{13}C ($CDCl_3$) δ 172.61, 104.77, 77.77, 71.70, 71.28, 70.59, 70.48, 70.40, 70.21, 70.17, 58.68, 55.81, 44.77, 28.65. IR (KBr) 3439, 2878, 2193, 2088, 1736, 1637, 1370, 1256, 1118 cm^{-1}. Anal. calc. for $C_{49}H_{27}NO_9D_{70}$: C, 64.34; H, 10.69; N, 1.53. Found: C, 64.65; H, 10.61; N, 1.51.].

Expression of Nef and dNef

Briefly, a fresh colony was selected and grown overnight in 25mL Luria broth (LB) at 37 °C and 200 rpm. The following day, this starter culture was diluted to 250 mL LB with the appropriate antibiotics and allowed to grow at 37°C and 200 rpm until OD_{600} = 0.6-0.8. Protein expression was induced by the addition of isopropyl β-D-1-thiogalactopyranoside (IPTG) to a final concentration of 1mM. Protein was expressed at 37 °C and 200 rpm for 4-6 hours. Cells were collected by centrifugation and stored at -80 °C until purification. For purification, the pelleted cells were resuspended in lysis buffer (20mM Tris, 100 mM NaCl, 20 mM imidazole, 10% glycerol, 5 mM β-mercaptoethanol (β-ME), pH 8.3) and lysed by sonication in the presence of

phenylmethylsulphonyl fluoride (PMSF) and lysozyme followed by centrifugation at 16,000 rpm at 4 °C. Ni-NTA Agarose (QIAGEN) was added to the clarified lysate and allowed to mix at 4 °C for at least one hour. A gravity flow-cell and UV detector (Pharmacia Biotech) were used to extensively wash the Ni-NTA agarose with lysis buffer and the protein was eluted with 20 mM Tris, 100 mM NaCl, 200 mM imidazole, 10% glycerol, 5 mM β-ME, pH 8.3. The eluate was dialyzed against 20 mM Tris, 100 mM NaCl, 5 mM β-ME, pH 8.3. The final concentration of protein was determined by the Bradford method and the mass confirmed by mass spectrometry. Expression of d-Nef was the same as above with the following exceptions: Bioexpress Cell Growth Media, U-D, 98% (Cambridge Isotope Laboratories, Inc.) was used instead of LB and the induction was carried out at 30 °C instead of 37 °C.

Measurement protocol on SPEAR and NG7

SPEAR is a time-of-flight spectrometer that operates at a fixed angle of incidence. A high flux and the fact that data for the entire range of q_z are collected simultaneously make this spectrometer particularly advantageous for rapid and time-dependent studies. However, for a liquid surface the q_z range is limited to ~ 0.15 $Å^{-1}$ by the fixed value of incident angle θ_i and the range of wavelength λ (2–16 Å) available from the spallation source. On NG7 a monochromator was used to select a wavelength of 4.76 Å. Tilting the monochromator makes available a wide range of θ_i, and data for each value of q_z is collected successively. A lower incident flux on the sample leads to substantially longer counting times compared with SPEAR, but the data extend to higher values of q_z (q_z = 0.23 $Å^{-1}$ is the mechanical limit of NG7). With an H_2O subphase there is no critical edge for total reflection, and absolute reflectivities were obtained on NG7 using a beam monitor. To put the data from SPEAR on an absolute scale, the same lipid solution was spread and measured on both SPEAR and NG7. The other reflectivity curves from SPEAR were then scaled to those data using the total beam current on target during the scans.

Investigations to achieve a monomolecular layer of membrane-bound Nef

Our initial NR measurements of 6His-d-Nef (henceforth d-Nef) bound to lipid membranes from solution at 0.5 μM revealed the presence of two layers: a ~ 40 Å dense layer immediately adjacent to the lipid head groups followed by a second layer that was substantially more dilute. This is shown in Fig S1, which displays NR data for d-Nef bound to a monolayer comprised of 65% h-DSIDA/Cu^{2+} + 35% h-DPPC (Fig S1a) and for d-Nef bound to a monolayer comprised of 65% h-DSIDA/Cu^{2+} + 35% d-DPPC (Fig S1b). The data for fully protonated lipid tails is more sensitive to the presence of the protein, but the data with d-DPPC extends to higher q_z values (and thus provides higher resolution). The two data sets were obtained at identical solution conditions and were collected after the changes in the NR data had become independent of time on the scale of several hours. Both data sets contain a shoulder at $q_z = 0.02$ $Å^{-1}$ ~ 0.03 $Å^{-1}$ revealing the presence of the more dilute second layer. This shoulder was not present upon first adsorption, but developed over time, as shown in supplementary Figs S2a and S2b.

The four data sets in Fig S1a and S1b were fit simultaneously, where only the SLD of the lipid tails was allowed to vary among the different SLD profiles to account for the different levels of deuteration. The SLD profiles with uncertainty limits are given in Fig S1c and Fig S1d. The profiles for the lipids alone are denoted by a cyan/blue/pink color scheme, and the profiles with d-Nef are denoted by a black/red/yellow color scheme. The mixture of 65% h-DSIDA/Cu^{2+} + 35% d-DPPC gives $SLD_{lipid\ tails}$ ~ 2 x 10^{-6} $Å^{-2}$, whereas for fully protonated lipids $SLD_{lipid\ tails}$~ -0.5 x 10^{-6} $Å^{-2}$. The profiles show that the SLD of the lipid headgroup region increases upon adsorption due to the insertion of d-Nef residues into the lipid headgroups. This is consistent with the fact that, for the present conditions, adsorption of d-Nef to the lipid monolayers is always accompanied by an increase in the area per molecule of ~5% as shown in Fig 3 of the main text. The profiles reveal the characteristics of the two layers formed by d-Nef. The initial layer is ~ 40-50 Å (full width at half max), has high occupancy (9.8 x 10^{-4} d-Nef molecules/$Å^2$), and is directly adjacent to the lipid headgroups. The second layer is roughly the same thickness,

but at much lower occupancy (1.6 x 10^{-4} d-Nef molecules/Å^2). We note that the second layer could not be removed by exchanging the subphase with pure Tris buffer (Fig S3). The fact that the dilute layer was not originally present upon first adsorption but developed over time suggests that it is due to a second layer of d-Nef that associated strongly to the original bound monolayer of d-Nef. Previous studies have reported that full length Nef is prone to aggregation above 100 μM at pH 8 (47, 48, 52). Dithiothreitol (DTT) is typically added at 5 mM to Tris buffer to inhibit association of Nef molecules through disulfide bonds. However, DTT could not be included in the present case because it inhibited binding of the His-tagged d-Nef to the model membrane by reducing Cu^{2+} to Cu^{+}.

Figure S4a displays NR data after allowing d-Nef to adsorb to 65% h-DSIDA/Cu^{2+} + 35% d-DPPC from solution at 0.5 μM for a period of 5 hrs, and also data collected after exchanging the subphase with Tris buffer containing 5 mM β-ME. The data sets are summations of three scans of ½ hour duration each. The data for adsorbed d-Nef in Fig S4a were collected after the reflectivity had become independent of time on the scale of several hours. The second layer was again clearly evidenced by a shoulder in the data at q_z = 0.02 Å^{-1} ~ 0.03 Å^{-1}. After exchanging the subphase with Tris buffer containing β-ME and then with pure Tris buffer, the shoulder was no longer evident, indicating that most or all of the second layer had been removed. The three data sets were fit simultaneously, where the SLD of the subphase and all characteristics of the lipid layers, except the headgroup SLD, were held constant. The results are shown in Fig S4b and Fig S4c. In this case the SLD of the lipid tails was slightly greater than that for the data in Fig S1b, although the monolayers were nominally the same composition. This reflects the strong sensitivity to small variations in the lipid composition, which could result from errors in weighing the powders or variations in the spreading process. The SLD profile in Fig S4b again indicates two layers of comparable thickness. After subphase exchange with Tris buffer containing 5 mM β-ME (Fig S4c), a layer of ~ 40 +/- 4 Å thickness remained with the maximum in residue density adjacent to the headgroups.

In work subsequent to that shown in Fig S4 we found that the second adsorbed layer of d-Nef could be largely avoided by arresting adsorption at an early stage. This was accomplished by exchanging the subphase with Tris buffer after a short period of d-Nef adsorption from a 0.5 μM solution concentration. Fig S5a shows reflectivity collected after allowing d-Nef to adsorb to a monolayer of 65% d-DSIDA/Cu^{2+} + 35% d-DPPC for 2.0 hrs from solution at 0.5 μM and then arresting adsorption by subphase exchange with pure buffer, and also data collected after exchanging the subphase again with 50 ml of Tris buffer containing 5 mM β-ME followed by 50 ml of pure Tris buffer. Since in this case both lipids were deuterated, the reflectivity was increased to the extent that the reflected intensity was well above the background at $q_z = 0.15$ $Å^{-1}$, the maximum q_z that can be attained on the SPEAR reflectometer for free liquid surfaces. The results from simultaneous fits of these three data sets using a model-independent multiple slab approach are shown in Fig S5b and Fig S5c. Adsorption of the second layer was largely avoided by exchanging the subphase with pure buffer after 2.0 hrs. Subsequent exchange of the subphase with Tris buffer containing 5 mM β-ME led to nearly complete removal of the second layer. The model-independent profile is comprised of a ~ 40 Å layer dense in residues that is directly adjacent to the lipid headgroups with only a very slight tail likely indicating a small residual amount of the second adsorbed layer. The dense layer is asymmetric with the maximum skewed toward the membrane.

We note that the appropriate concentration of β-ME for use in exchanging the subphase can vary with the age of the material. In the runs corresponding to the data in Fig S4 and Fig S5, a vial of β-ME was used that was several years old. For fresh β-ME, the same concentration removed most of the protein from the membrane (data not shown). For this reason a lower concentration of β-ME was used in the run corresponding to the data in Fig 2 of the main text.

Fig S6 compares the results for nominally identical runs performed on SPEAR (LANL) and on NG7 (NIST).

The second adsorbed layer could also be largely avoided by using a lower bulk concentration of d-Nef. Reflectivity data are shown in Fig S7 for d-Nef adsorbed to 65%

d-DSIDA/Cu^{2+} + 35% d-DPPC from solution at 0.2 μM. In this case adsorption was allowed to proceed for 6 hrs, at which point little change was observed in repeated scans. In this case the subphase was not exchanged prior to collecting the final reflectivity data. The reflectivity data are shown in Fig S7a and the results of simultaneous fits to the data before and after adsorption of d-Nef are shown in Fig S7b. Only a very dilute second layer was present. However, the coverage of the first layer was substantially lower than when d-Nef adsorbed from solution at 0.5 μM.

Effect of exchanging the subphase with buffer containing 0.5 mM β-ME for the run corresponding to Figure 2 in the main text

Figure S8 shows the effects of exchanging the subphase with buffer containing 0.5 mM β-ME for the same run as in Fig 2 of the main text. Very little change in the reflectivity was observed upon subpahse exchange. In particular, the shoulder at q_z = 0.026 $Å^{-1}$ corresponding to the second adsorbed layer was unaffected. The fact that a small amount of the second layer remained probably indicates that the concentration of β-ME was too low.

Average SLD profile for conformations in the simulated ensemble with distance between the center of the globular domain and the center of the His tag in the range of 10-20 Å

Figure S9 compares the calculated reflectivity (a) and average SLD profile (b) for all conformations of the ensemble for which the distance between the center of the globular domain and the center of the His tag falls in the range of 10-20 Å, along with the experimental results. The vast majority (~ 99%) of the conformations in the ensemble do not reproduce the combination of asymmetry and breadth of the main peak in the experimental profile.

Binding in the absence of interaction through the N-terminal His tag

Figure S10 shows NR data for a case in which 5 mM DTT was present in the buffer from the start. This study involved binding of d-Nef at 0.5 uM to 65% h-DSIDA/Cu^{+} + 35% h-

DPPC where Cu^{2+} was originally loaded into the DSIDA headgroups but was reduced to Cu^{+} by DTT. This abolished binding through the His tag. Protonated lipids were used in order to detect the low level of binding of d-Nef in this case. This limited the range of q_z to 0.10 $Å^{-1}$ and consequently little detail of the profile could be determined.

Lack of area change upon binding of 10His-MD2 to a DSIDA/Cu^{2+}-containing membrane

MD2 is an accessory protein in the mammalian innate immune system and its binding through a 10His tag to DSIDA/Cu^{2+}-containing membranes was studied in prior work (unpublished). Figure S11a shows NR data for 10His-MD2 at 6 μM binding to 65% h-DSIDA/Cu^{2+} + 35% d-DPPG at 25 mN/m. Adsorption was barely detectable in the NR data at 4 μM (not shown), but was clearly evident at 6 uM. Little or no change in the surface area occurred upon binding, as shown in Figure S11b. The lack of change in surface area upon binding contrasts with the sharp increase in area upon binding of 6His d-Nef to 65% d-DSIDA/Cu^{2+} + 35% d-DPPC shown in Fig 3 of the main text. For the experiments in Fig S11, the subphase consisted of 40 mM phosphate buffered saline pH 7.2 with 100 mM NaCl maintained at 20 ºC.

Insertion of melittin into Langmuir monolayers of DPPC detected through increase in area per molecule

Figure S12 shows that the area per molecule in DPPC monolayers increases with concentration of melittin (Sigma-Aldrich) in the subphase. The subphase consisted of 40 mM phosphate buffered saline pH 7.2 with 100 mM NaCl maintained at 20 ºC.

NR data plotted in standard form

Fig S13 shows the data of Fig 2a of the main text plotted as reflectivity versus q_z. At the highest q_z values, the error bars are comparable to the size of the symbols.

a)

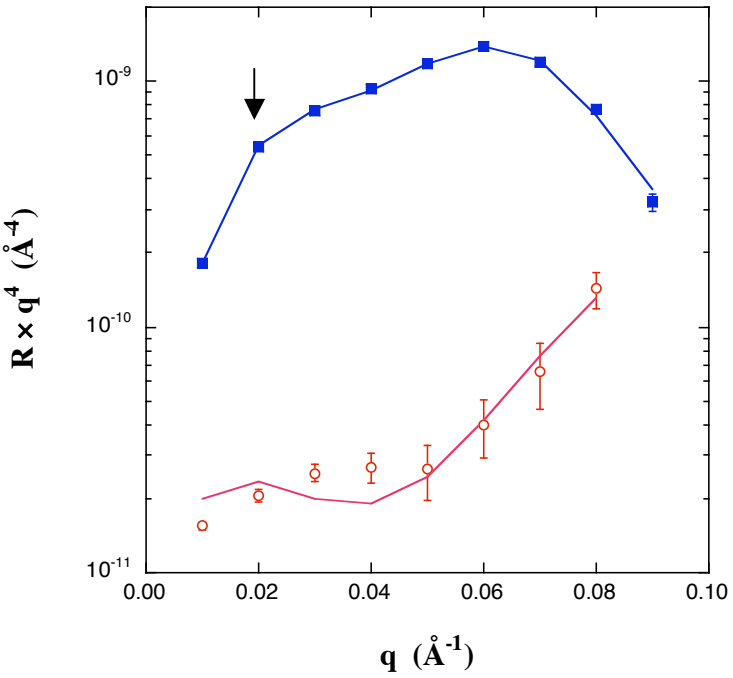

b)

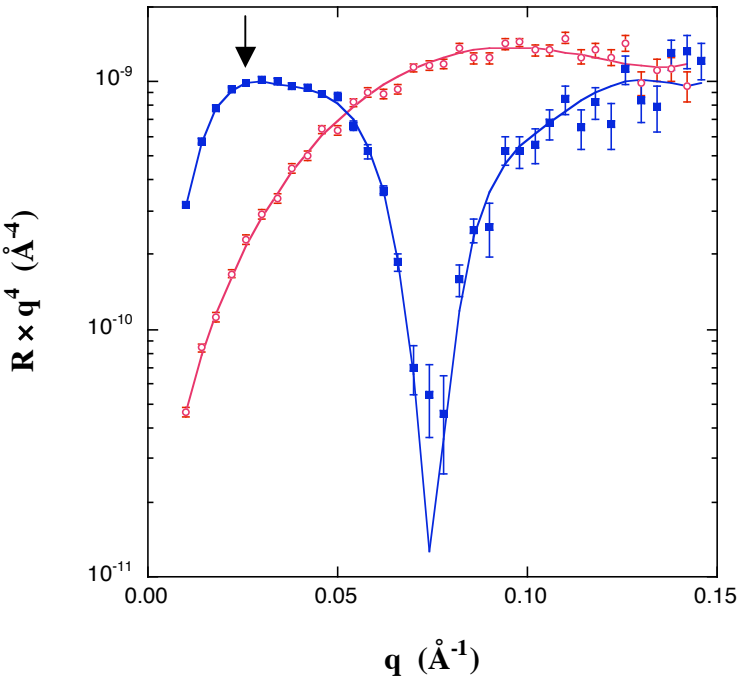

Figure S1. NR data for lipid monolayer alone (○) and with bound d-Nef (■) for lipid monolayer comprised of a) 65 % h-DSIDA/Cu^{2+} + 35% h-DPPC and b) 65 % h-DSIDA/Cu^{2+} + 35% d-DPPC. The arrows highlight a shoulder in each data set that is indicative of a second d-Nef layer. The solid curves are the result of simultaneous fits to all four data sets as described in the text.

c)

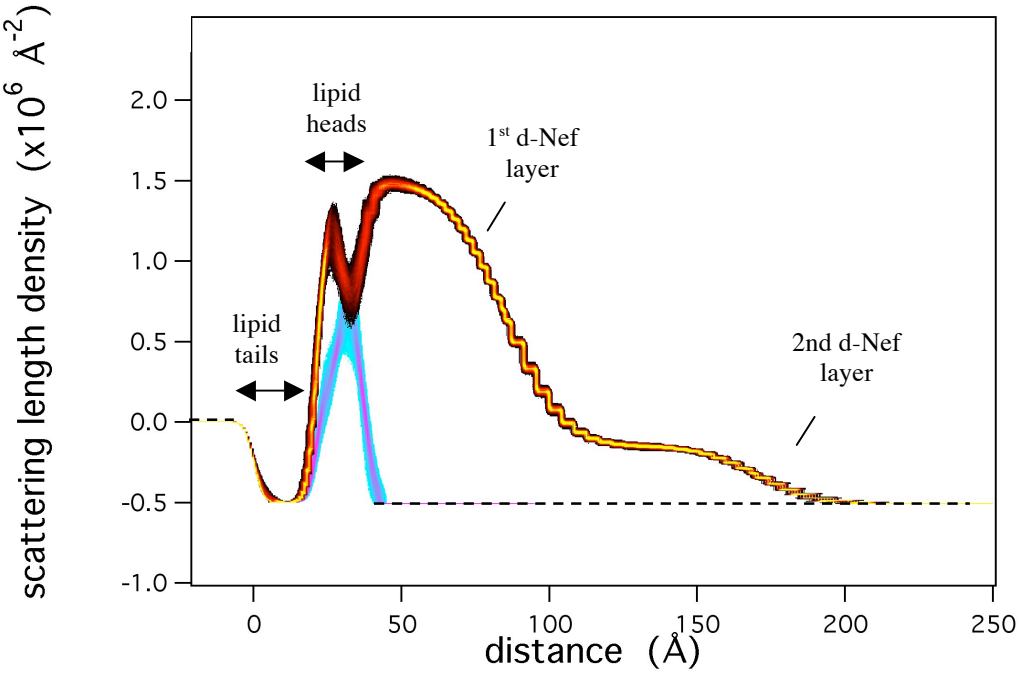

d)

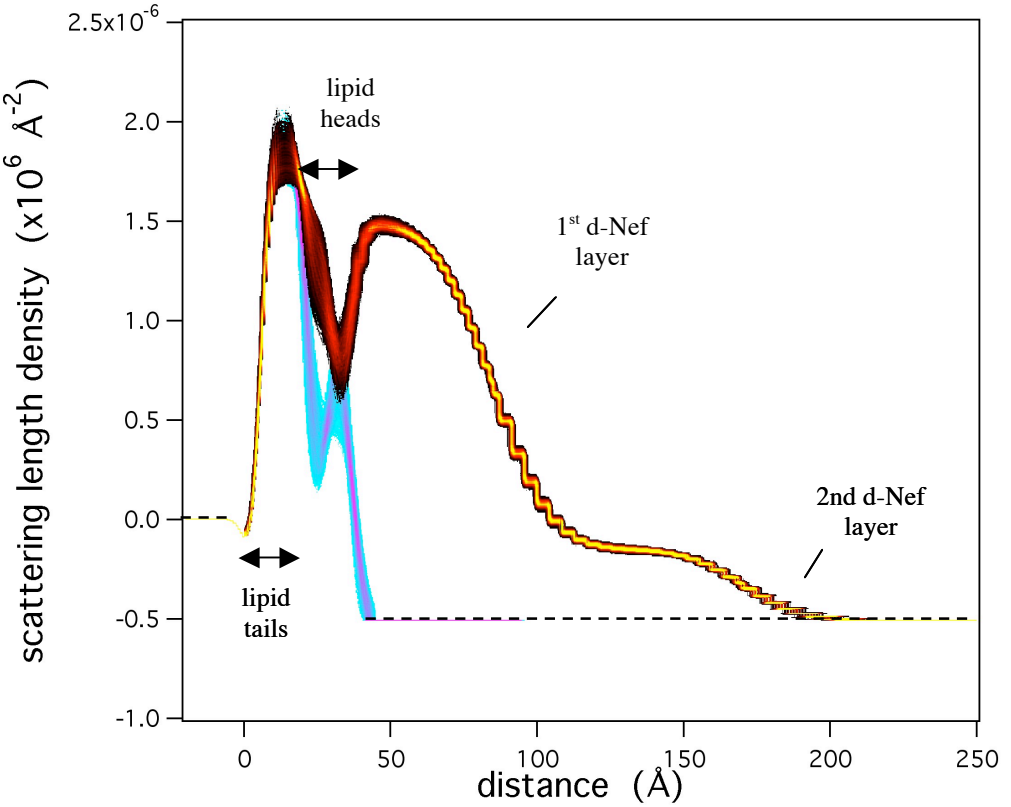

Figure S1 (continued). c) SLD profiles for d-Nef bound to 65 % h-DSIDA/Cu^{2+} + 35% h-DPPC. The profiles for the lipids alone are shown in blue/pink, and the profiles with d-Nef are shown in black/red/yellow. d) SLD profiles for d-Nef bound to 65 % h-DSIDA/Cu^{2+} + 35% d-DPPC.

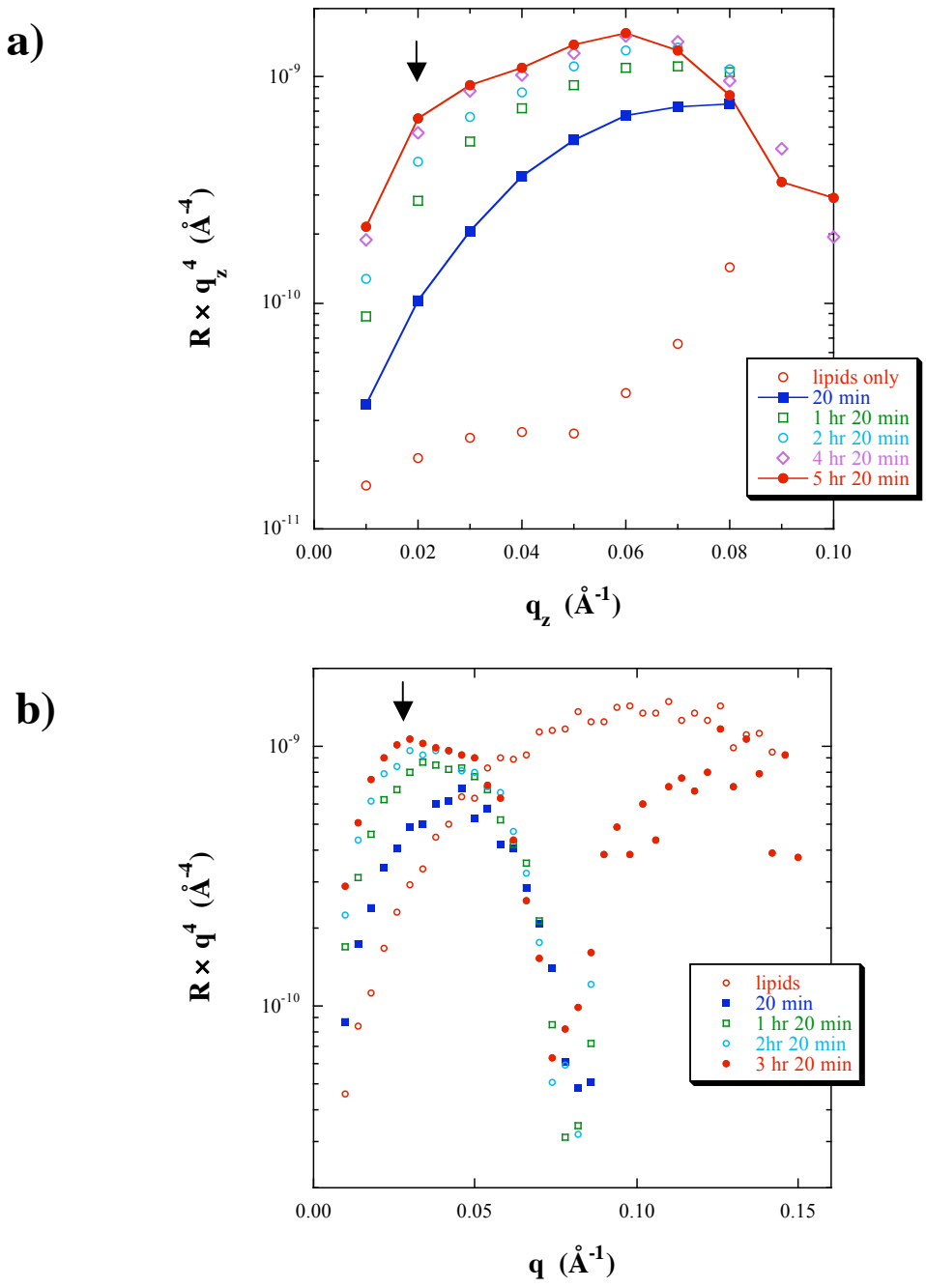

Figure S2. Time dependent changes in the reflectivity curves prior to reaching the time-independent data shown in Figure 2 of the main text. The arrows indicate a shoulder that develops over time in the data for a) 65 % h-DSIDA/Cu^{2+} + 35% h-DPPC and (b) 65 % h-DSIDA/Cu^{2+} + 35% d-DPPC. This feature corresponds to the development of a second layer of adsorbed d-Nef.

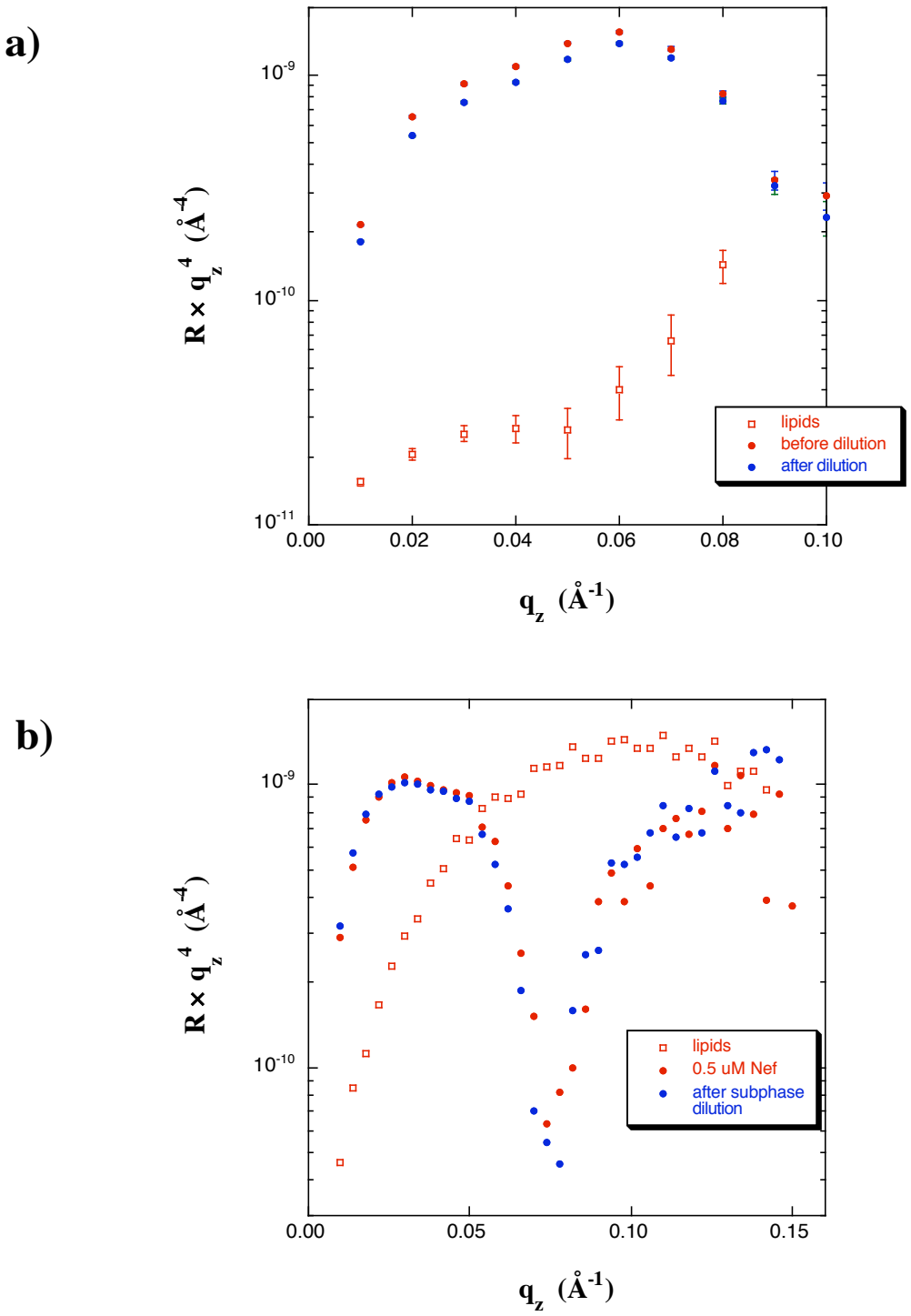

Figure S3. NR data for lipid monolayer alone and with bound d-Nef for lipid monolayer comprised of a) 65 % h-DSIDA/Cu^{2+} + 35% h-DPPC and (b) 65% h-DSIDA/Cu^{2+} + 35% d-DPPC. Also shown are data after exchanging the subphase with buffer. The data show that the second adsorbed layer does not desorb upon exchanging the subphase with pure buffer.

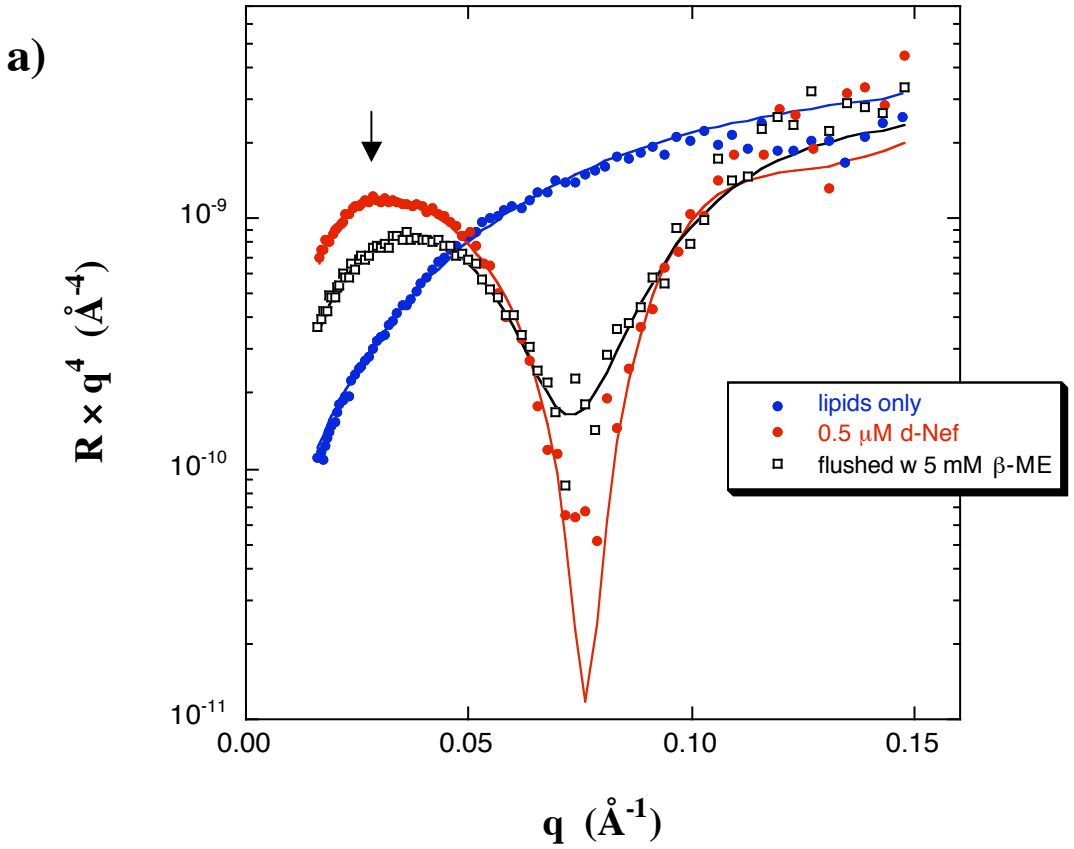

Figure S4. (a) NR data for a 65% h-DSIDA/Cu^{2+} + 35% d-DPPC monolayer alone, with bound d-Nef, and then after exchanging the subphase with Tris buffer containing 5 mM β-ME. Subphase exchange with buffer containing β-ME removed most of the second layer.

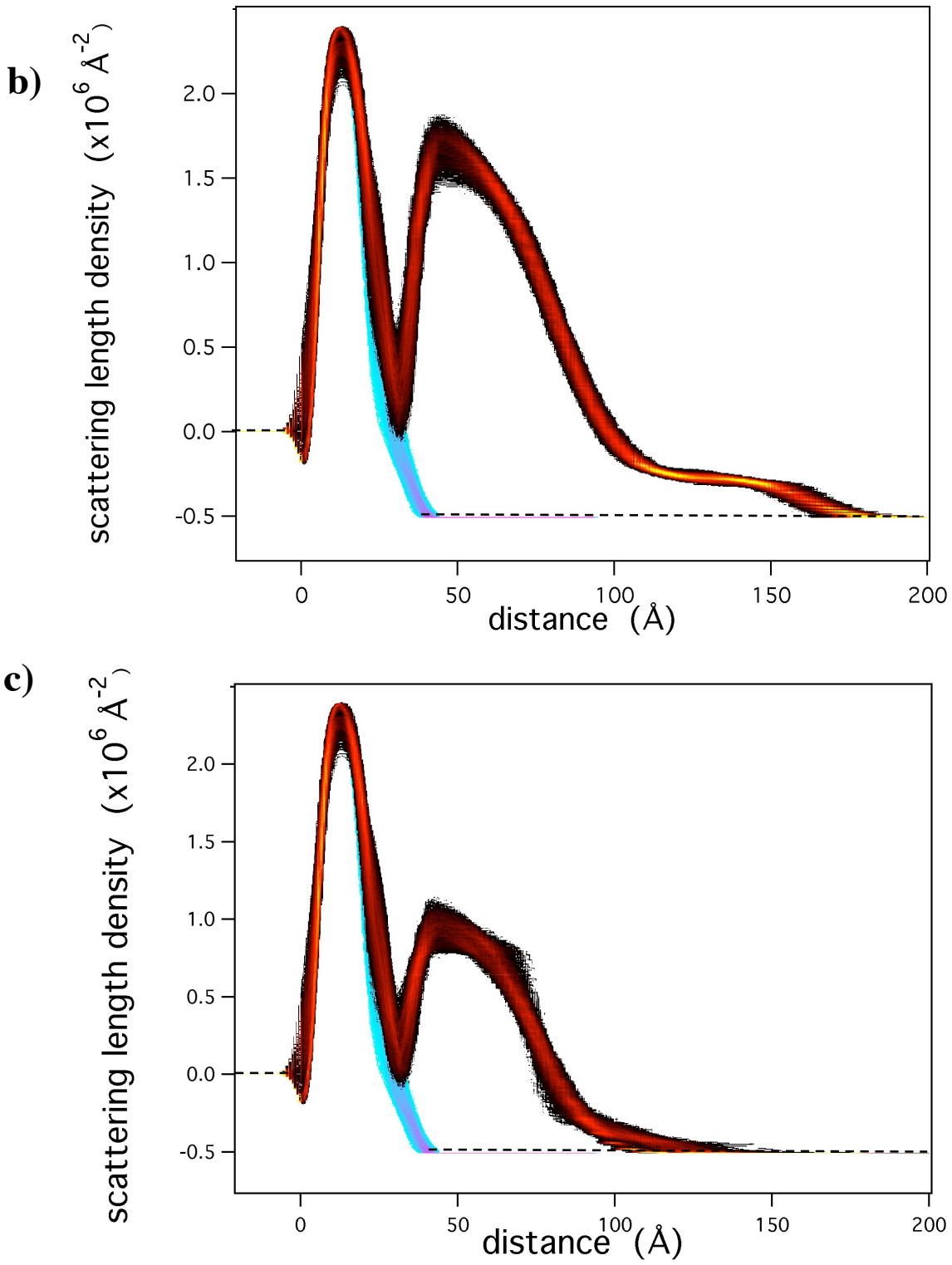

Figure S4 (continued). SLD profiles for (b) d-Nef bound to 65% h-DSIDA/Cu^{2+} + 35% d-DPPC and (c) after exchanging the subphase with Tris buffer containing 5 mM β-ME. Exchanging with buffer containing β-ME removed most of the second layer.

a)

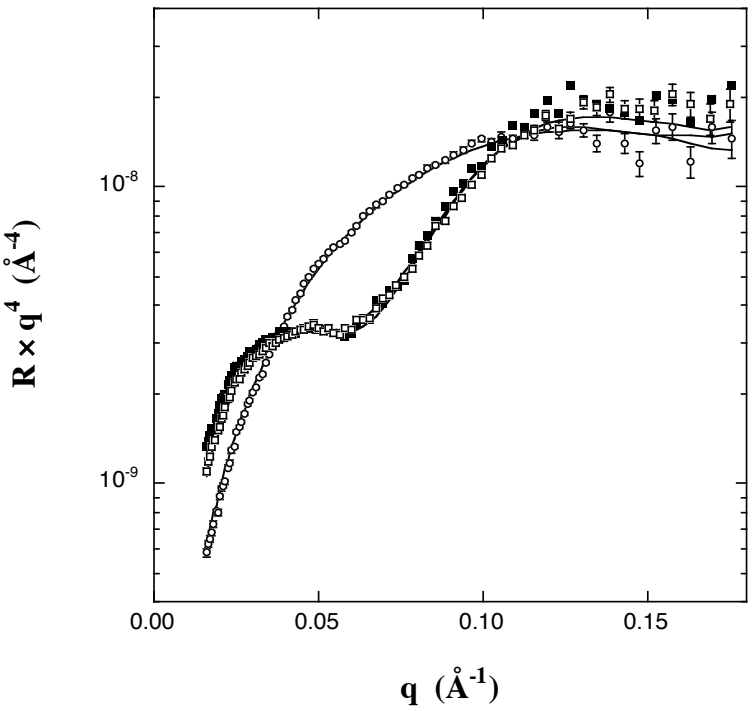

Figure S5. a) NR data for a 65% d-DSIDA/Cu^{2+} + 35% d-DPPC monolayer alone (○), after injecting d-Nef at 0.5 μM and allowing adsorption to proceed for 2.0 hrs (□), and then after exchanging the subphase with Tris buffer containing 5 mM β-ME (■).

b)

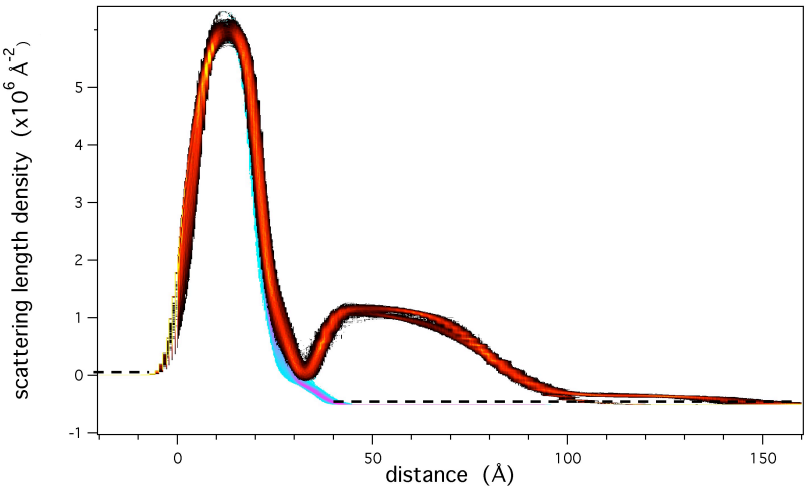

c)

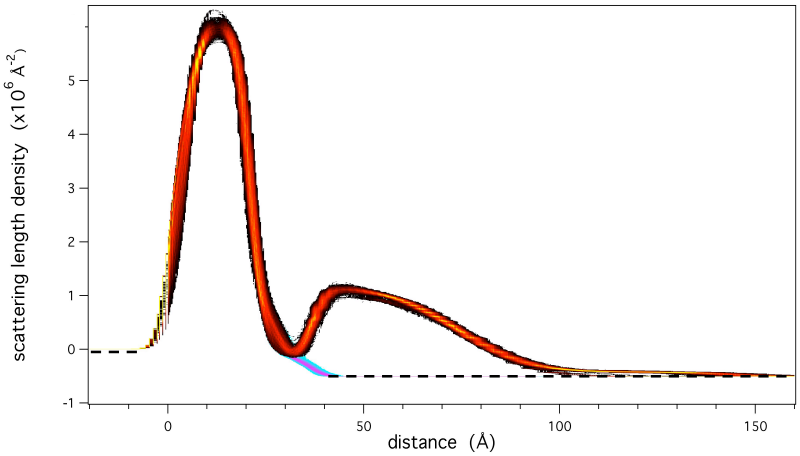

Figure S5 (continued). b) SLD profile obtained after injecting d-Nef at 0.5 μM under a 65% d-DSIDA/Cu^{2+} + 35% d-DPPC monolayer and allowing adsorption to proceed for 2.0 hrs. c) SLD profile obtained after exchanging the subphase with Tris buffer containing 5 mM β-ME. Arresting adsorption after 2.0 hrs eliminated nearly all of the second adsorbed layer.

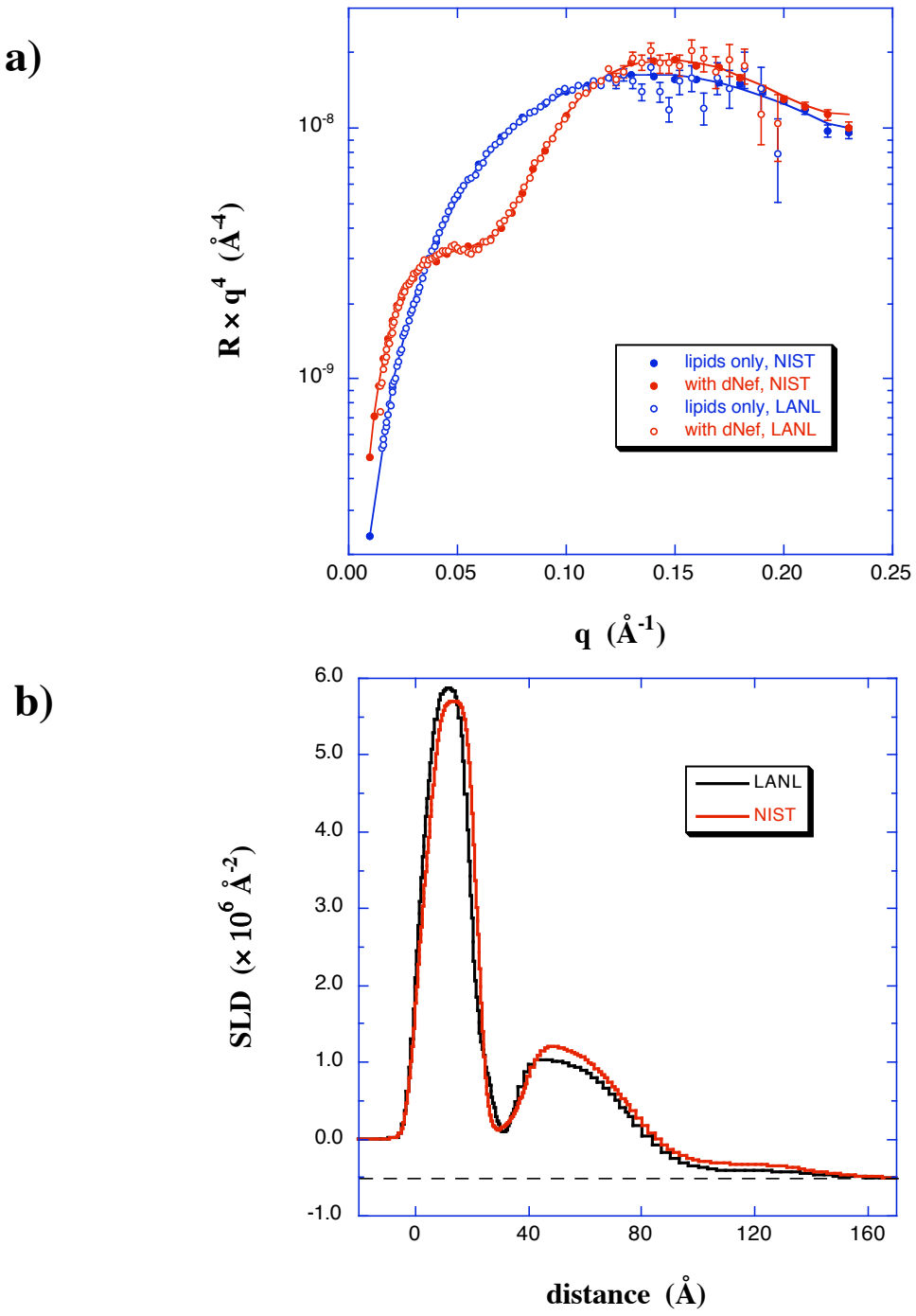

Figure S6. a) Comparison of data obtained on SPEAR (LANL) and on NG7 (NIST) under nominally identical conditions. The latter is from Fig 2a of the main text. The data from SPEAR show a slight maximum at q = 0.048 Å^{-1}followed by a slight minimum at q = 0.056 Å-1, indicating that less of the second layer is present. b) Comparison of the profiles from the data in a).

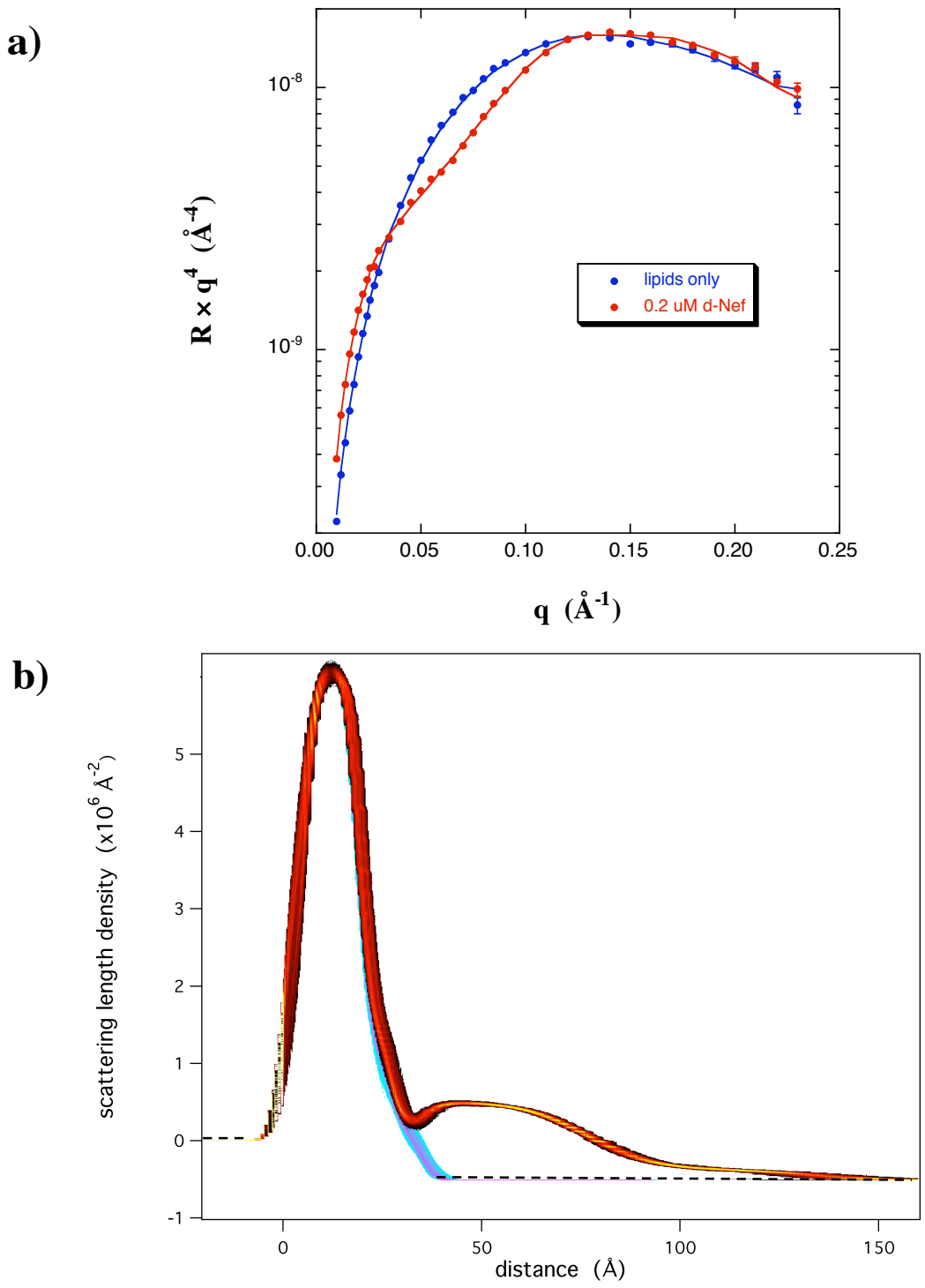

Figure S7. a) NR data for a 65% d-DSIDA/Cu^{2+} + 35% d-DPPC monolayer alone (○) and with bound d-Nef (●) adsorbed from solution at 0.2 μM. Adsorption was allowed to proceed for 6 hrs. b) SLD profiles corresponding to the data in (a).

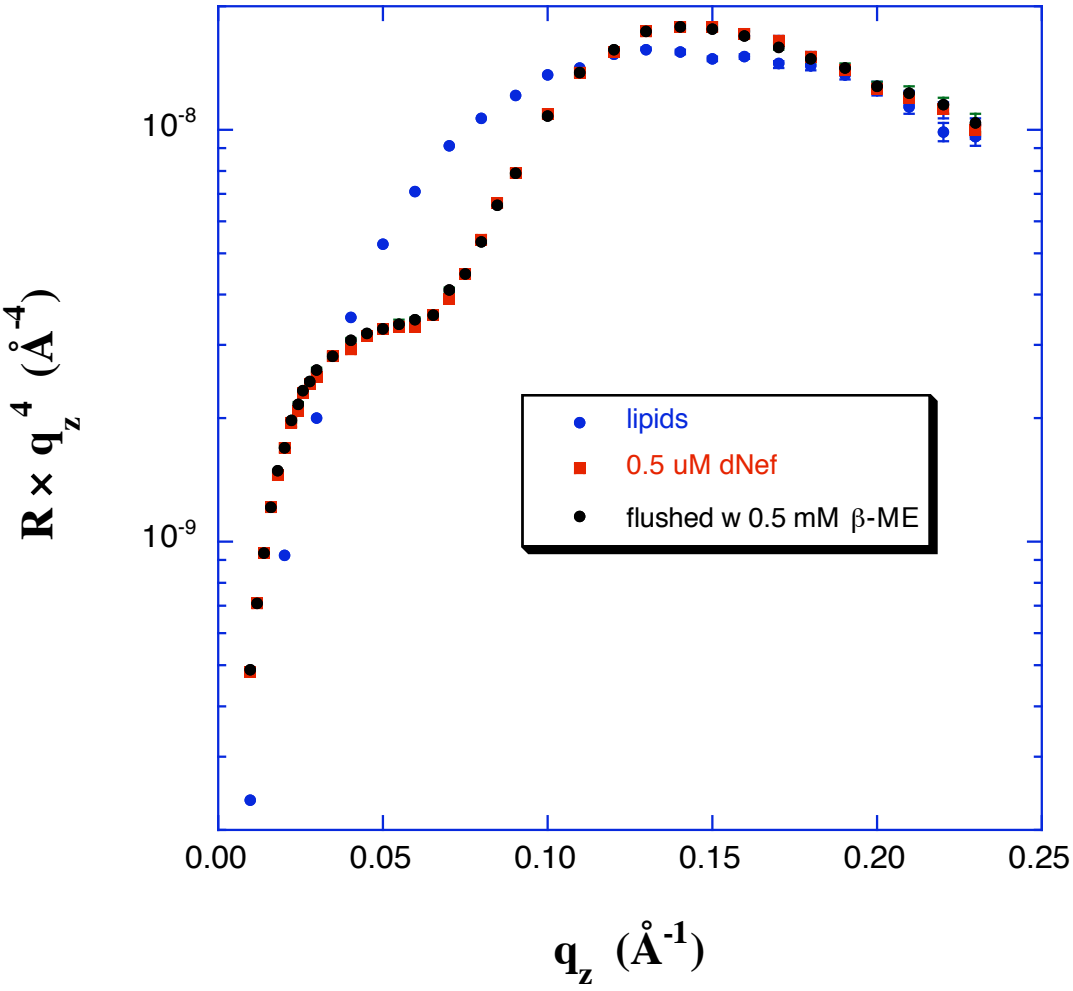

Figure S8. a) NR data for the run shown in Fig 2 of the main text showing that very little change was observed after exchanging the subphase with 0.5 mM β-ME.

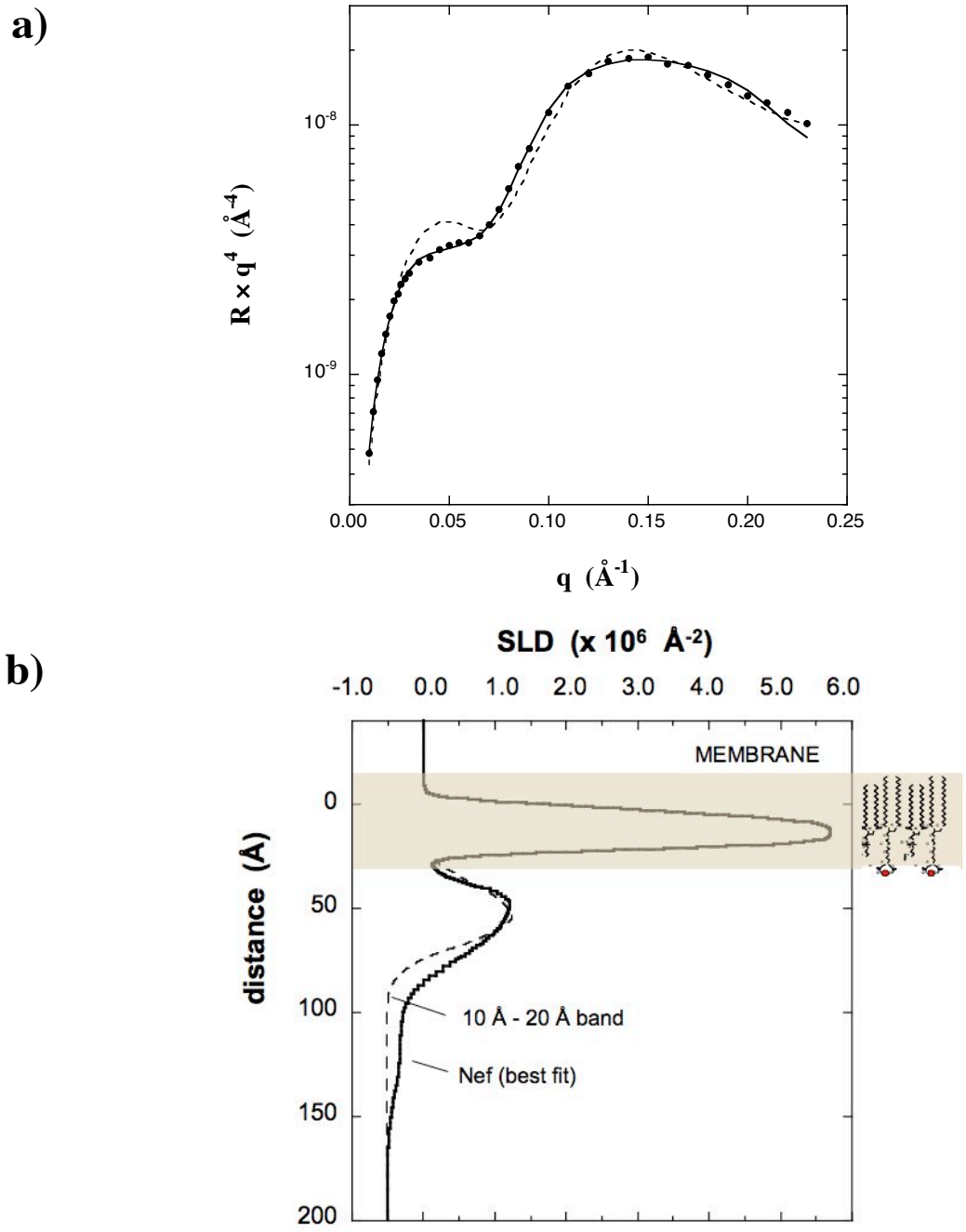

Figure S9. Calculated reflectivity a) and average SLD profile b) for simulated conformations in which the distance between the center of the globular domain and the center of the His tag ranges from 10 – 20 Å, along with the experimental results. For the average SLD profile from the simulated conformations, the breadth of the main peak is narrower than for the experimental profile and does not contain the asymmetry of the experimental profile.

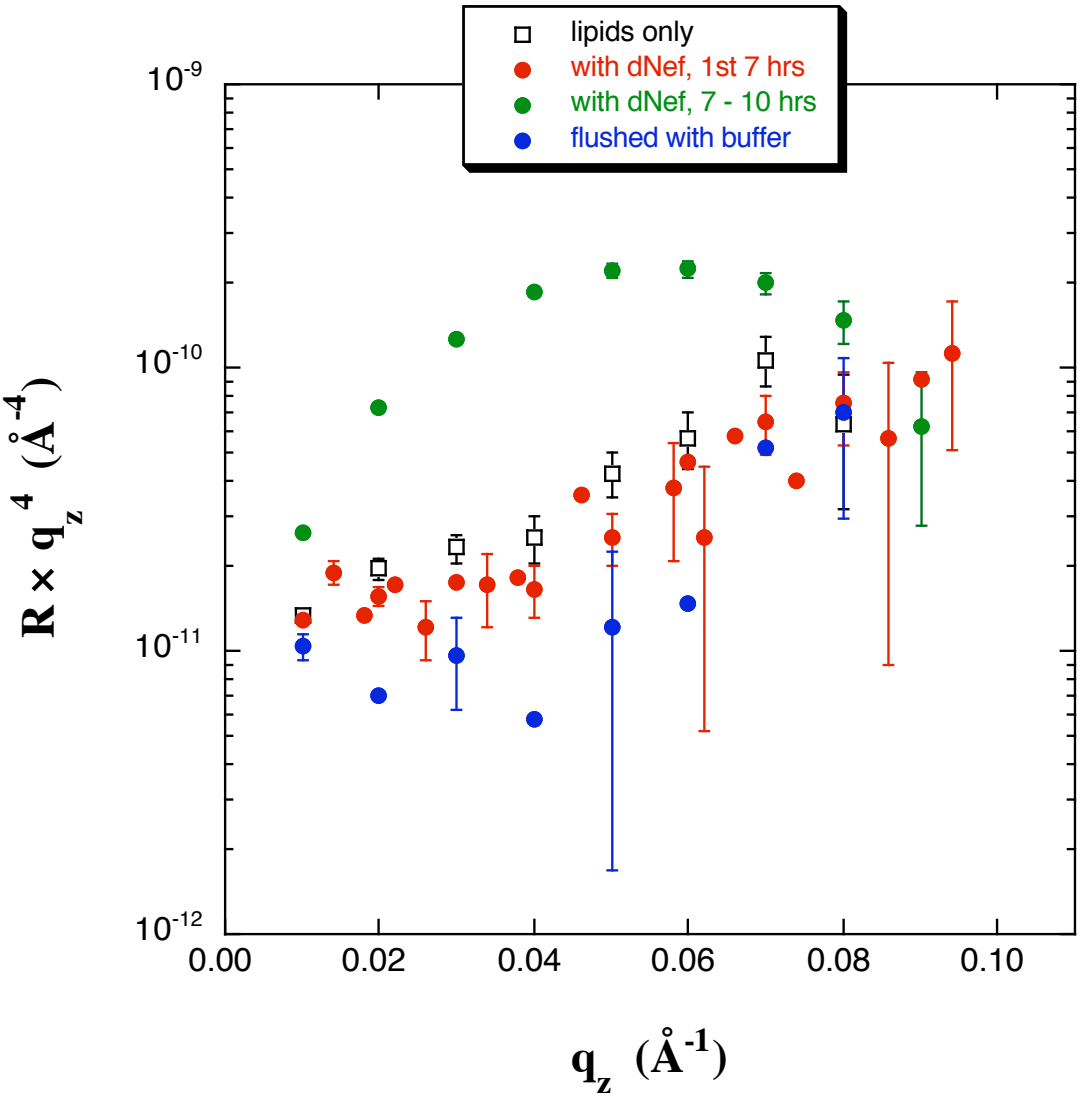

Figure S10. NR data for a 65% h-DSIDA/Cu^{2+} + 35% h-DPPC monolayer with 5 mM DTT in the buffer (□), data collected during the first 7 hrs after introducing 0.5 uM dNef into the subphase (●), data collected from 7 - 10 hrs after introducing 0.5 uM dNef (●), and data obtained after exchanging the subphase with buffer (●).

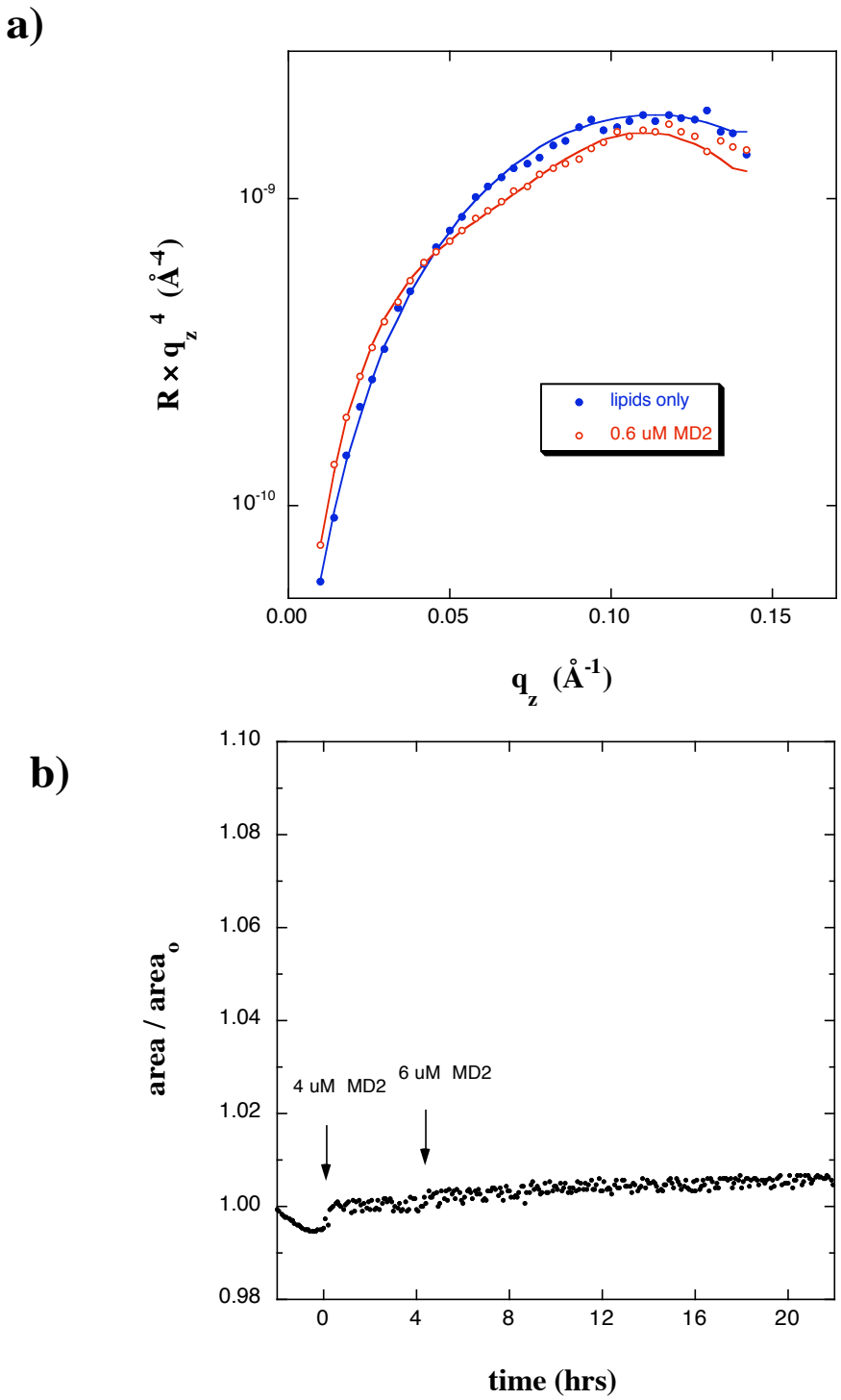

Fig S11. a) NR data for 10His-MD2 at 6 μM binding to 65% h-DSIDA/Cu^{2+} + 35% d-DPPG at 25 mN/m. Adsorption was barely detectable in the NR data at 4 μM (not shown), but was clearly evident at 6 uM. b) Surface area data corresponding to the NR data in a). The lack of change in surface area upon binding of 10His-MD2 to 65% h-DSIDA/Cu^{2+} + 35% d-DPPG contrasts with the sharp increase in area upon binding of 6His Nef to 65% d-DSIDA/Cu^{2+} + 35% d-DPPC shown in Fig 3 of the main text.

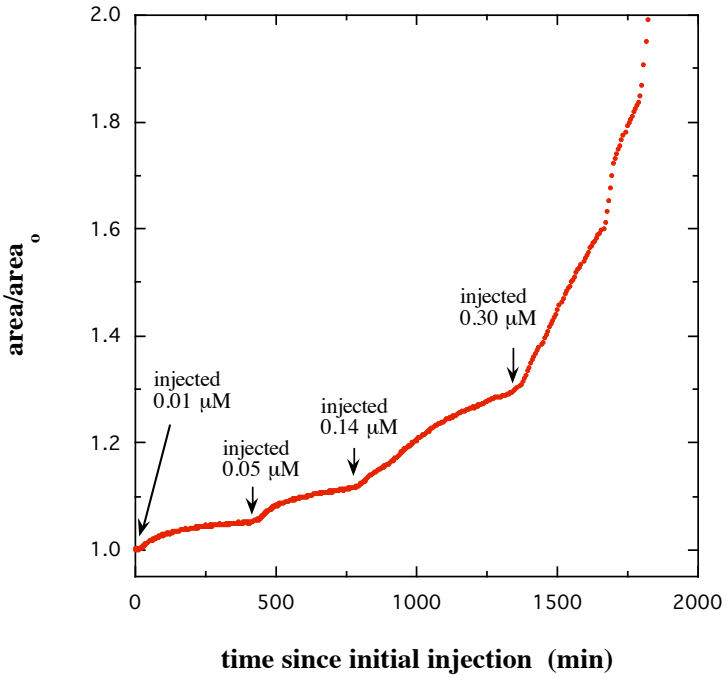

Figure S12. Area change upon injection of melittin underneath a Langmuir monolayer of DPPC maintained at a surface pressure of 30 mN/m. The increase in area with melittin concentration indicates insertion into the monolayer.

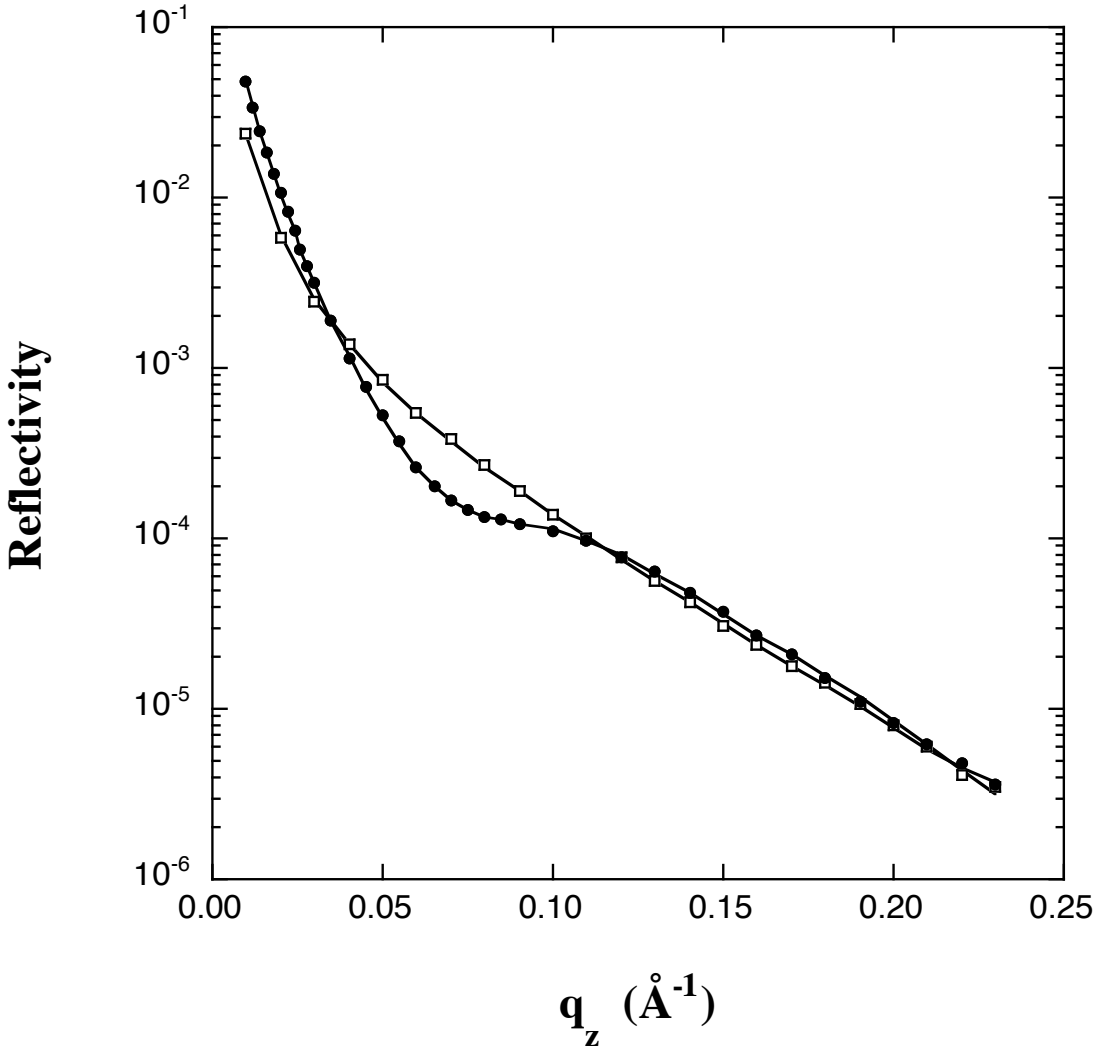

Fig S13. Data of Fig 2a of the main text plotted as reflectivity versus q_z. At the highest q_z values, the error bars are comparable to the size of the symbols.